AIP Advances

Effect of crystal structure and cationic order on phonon modes across ferroelectric phase transformation in Pb(Fe0.5-xScxNb0.5)O3 bulk ceramics

B. Mallesham, B. Viswanath, and R. Ranjith

Citation: AIP Advances **6**, 015116 (2016); doi: 10.1063/1.4941341
View online: http://dx.doi.org/10.1063/1.4941341
View Table of Contents: http://scitation.aip.org/content/aip/journal/adva/6/1?ver=pdfcov
Published by the AIP Publishing

Effect of crystal structure and cationic order on phonon modes across ferroelectric phase transformation in $Pb(Fe_{0.5-x}Sc_xNb_{0.5})O_3$ bulk ceramics

B. Mallesham,[1] B. Viswanath,[2] and R. Ranjith[1,a]
[1]*Department of Materials Science and Metallurgical Engineering, Indian Institute of Technology Hyderabad, Kandi, Sangareddy - 502285, Telangana, India*
[2]*School of Engineering, Indian Institute of Technology Mandi, 175001, Himachal Pradesh, India*

(Received 10 November 2015; accepted 20 January 2016; published online 29 January 2016)

$Pb(Fe_{0.5-x}Sc_xNb_{0.5})O_3$ [(PFSN) ($0 \leq x \leq 0.5$)] multiferroic relaxors were synthesized and the temperature dependence of phonon modes across ferroelectric to paraelectric transition was studied. With varying Sc content from x = 0 to 0.25 the structure remains monoclinic and with further addition (x = 0.3 - 0.5) the structure transforms into rhombohedral symmetry. Structural refinement studies showed that the change in crystal structure from monoclinic to rhombohedral symmetry involves a volume increment of 34-36%. Associated changes in the tolerance factor ($1.024 \leq t \leq 0.976$) and bond angles were observed. Structure assisted B′-B″ cation ordering was confirmed through the superlattice reflections in selected area electron diffraction (SAED) pattern of $Pb(Sc_{0.5}Nb_{0.5})O_3$ (x = 0.5). Cation ordering is also evident from the evolution of Pb-O phonon mode in Raman spectra of compositions with rhombohedral symmetry ($x \geq 0.3$). The high temperature Raman scattering studies show that the B-localized mode [F_{1u}, ~ 250 cm^{-1}] and BO_6 octahedral rotational mode [F_{1g}, ~ 200 cm^{-1}], both originating from polar nano regions (PNRs) behave like coupled phonon modes in rhombohedral symmetry. However, in monoclinic symmetry they behave independently across the transition. Softening of B localized mode across the transition followed by the hardening for all compositions confirms the diffusive nature of the ferroelectric transformation. The presence of correlation between the B localized and BO_6 rotational modes introduces a weak relaxor feature for systems with rhombohedral symmetry in PFSN ceramics, which was confirmed from the macroscopic dielectric studies. [http://dx.doi.org/10.1063/1.4941341]

I. INTRODUCTION

Relaxor ferroelectrics [General formula: $A(B'B'')O_3$] are special class of ferroelectrics, which exhibit (a) high dielectric constant (b) diffused phase transition (c) frequency dispersion in T_{max} (Temperature corresponding to dielectric maxima) and (d) weak remnant polarization.[1] The aforementioned phenomenological properties of relaxors are attributed to structural and chemical inhomogeneity due to random occupancy of B′ and B″ cations at B-site.[2,3] Certain relaxor ferroelectrics like $Pb(Sc_{0.5}Ta_{0.5})O_3$ (PST), $Pb(Sc_{0.5}Nb_{0.5})O_3$ (PSN) possess two different local nano regions namely: (a) polar nano regions (PNR) of lower symmetry (ferroic) (b) B′-B″ cation ordered regions (COR) of Fm-3m symmetry (non-ferroic).[1] The formation of PNRs in relaxors is attributed to the cation off center displacement and their re-orientational motion.[4] However, in relaxors CORs are believed to be structurally driven due to the difference in B′ and B″ cation ionic radius.[5,6] It is known that there exists a critical range of size for the chemically ordered regions (2-50 nm) to

[a]Corresponding author email: ranjith@iith.ac.in

exhibit relaxor features.[7] Moreover, from the phenomenological aspects there are four characteristic temperatures associated with PNRs of relaxor ferroelectrics such as T_d, T^*, T_m and T_f.[2] T_d is the burn temperature at which nucleation of PNRs begins,[8] T^* is known as intermediate temperature at which correlation between PNRs begins and merges to form larger size PNRs, T_m the temperature corresponding to dielectric maxima and T_f known as freezing temperature below which, the PNRs are frozen.[2] There are extensive studies on relaxors like $Pb(Mg_{0.33}Nb_{0.67})O_3$ (PMN), $Pb(Sc_{0.5}Nb_{0.5})O_3$ (PSN) and $Pb(Sc_{0.5}Ta_{0.5})O_3$ (PST) and their solid solutions with $PbTiO_3$ (PT) to understand the local structure and the interplay between different local nano regions like PNRs and CORs.[9,10] The locally embedded PNRs possess different size and shape with a dynamic character i.e., within micro-seconds these polar clusters with variable orientation originate and get annihilated.[8,11,12] Since, the dynamics of PNR in relaxors are strongly related to the lattice dynamics of the system, Raman scattering is a powerful tool to study the microscopic origin of the phenomenon observed in these relaxors.[11,12]

Recently multiferroic relaxors [$Pb(Fe_{0.5}Nb_{0.5})O_3$ (PFN), $Pb(Fe_{0.5}Ta_{0.5})O_3$, $Pb(Fe_{0.67}W_{0.33})O_3$] have attained great interest due to their structural similarity like conventional relaxors. Among these Lead Iron Niobate [$Pb(Fe_{0.5}Nb_{0.5})O_3$ (PFN)] is a single phase multiferroic compound, classified under mixed perovskite category of type – I multiferroics.[13] PFN was discovered by Smolenskii et al., in the early 1960' s. which exhibits ferroelectric transition (T_{max}) around 380 K and antiferromagnetic phase transition (T_N) around 143 K.[14–16] The presence of weak magnetoelectric coupling in PFN has been evidenced via observed anomalies in magnetic susceptibility around ferroelectric transition,[17] and dielectric anomalies around magnetic transition.[18] Hence, PFN is considered as one of the interesting single phase multiferroic compound to explore the fundamental science associated to its structure and properties. However, microscopic understanding of PFN is still challenging due to complex local structure and needed further investigation. This study focuses on the high temperature Raman scattering of $Pb(Fe_{0.5-x}Sc_xNb_{0.5})O_3$ ($0 \le x \le 0.5$) solid solutions to understand the role of structure and associated phonon mode behavior in the phase transition characteristics.

II. EXPERIMENTAL DETAILS

$Pb(Fe_{0.5-x}Sc_xNb_{0.5})O_3$ (x = 0, 0.1, 0.15, 0.2, 0.25, 0.3, 0.4, 0.5) ceramic powders were synthesized via solid state reaction route. The detailed synthesis procedure could be found elsewhere.[5] The structural and phase purity of the synthesized compounds was verified through X- ray diffraction technique [Make: PANalytical: Model: X-pert Pro]. TEM investigations were performed using FEI, Techani-T-20 operated at 200 kV. Electron transparent samples were prepared by mechanical polishing followed by argon ion milling with incident beam angle 5° and beam voltage 4 kV. Dielectric measurements of all the compounds were carried out using impedance analyzer (Make: Agilent, Model: 4294A). Raman spectra of the all the compositions from the ambient to 723K have been recorded using Dispersive Raman Microscope Spectrometer (Make: Bruker, Model: SENTERRA) attached with a heating stage (Make: Linkam, model: THMS 600).

III. RESULTS AND DISCUSSION

Rietveld refinement of our structural analysis confirmed that compositions containing Sc content $x \le 0.25$ exhibits a monoclinic crystal symmetry (space group: Cm) whereas $x > 0.25$ exhibit Rhombohedral crystal symmetry (space group: R3m) and the details of the structural refinement has been reported earlier.[5] The variations observed in the unit cell volume and bond angle ($B'/B'' - O - B'/B''$) with varying Sc content indicates structural transformation is like a first order phase transition from monoclinic to rhombohedral [Figure 1(a)]. Figure 1(a) shows the angle between B cation and oxygen at apical and planar positions of the octahedra in compounds with monoclinic symmetry (Cm). Whereas, compositions that exhibit rhombohedral symmetry (R3m) there is no such distinction between angles of apical and planar oxygen atoms exists. At lower Sc content $x \le 0.25$ the structure is stabilized in monoclinic phase with a small increment in unitcell volume, whereas at higher Sc content $x \ge 0.3$ structure is stabilized in rhombohedral phase as a

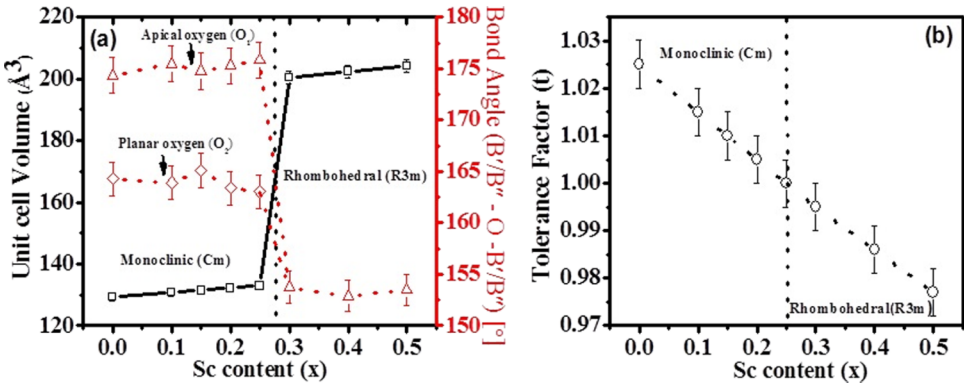

FIG. 1. (a) Change in unitcell volume and B′/B″ – O – B′/B″ bond angle with increasing Sc content from x = 0-0.5 in $Pb(Fe_{0.5-x}Sc_x)Nb_{0.5}O_3$ compounds (b) Variation of Tolerance factor (t) with increasing mol% of Sc in $Pb(Fe_{0.5-x}Sc_x)Nb_{0.5}O_3$ compounds (broken and solid lines connecting the data are guide to eyes in both (a) and (b)).

result volume of unit cell increases by 34-36% (figure 1(a)). Moreover, there is a drastic decrement in B′/B″-O-B′/B″ apical bond angle from ≈ 175° to 153° during the structural modification takes place at x = 0.3 mol% Sc. Similarly the bond angles of planar oxygen atoms decreases from ≈ 164° to 153°. Such decrement in the bond angles arises due to the B cation displacement along the <111> direction, eventually leads to a volume change across the compositions studied. Interestingly, PFN is known to suffer similar volume change and structural transformation under external pressure and in addition similar structures when substituted with cations of different ionic radius do suffer change in the B-cation distortions.[6,19] In the present case, sufficiently substituted amount of Sc (x = 0.3 mol %) exerts equivalent chemical pressure required for volume change (34-36%) and the structural modification from monoclinic to rhombohedral.

Moreover, geometrical packing and stabilization of perovskite structure can be described by Goldschmidt tolerance factor. A perovskite structure is known to stabilize at different crystal symmetry based on the value of tolerance factor.[20] The dependence of temperature coefficient of dielectric permittivity and morphotrophic phase boundary (MPB) of piezoelectric ceramics on tolerance factor has been studied extensively.[20–22] For example the value of tolerance factor at MPB compositions is around 0.990 – 0.993 for $Bi_{0.5}Na_{0.5}TiO_3$ based solid solutions and is independent of the amount of similar perovskite structures substituted in the parent lattice.[20] In the case of $Pb(Fe_{0.5-x}Sc_xNb_{0.5})O_3$ (PFSN) [$0 \le x \le 0.5$] ceramics the effective B-site ionic radius was calculated using the following equation.[23]

$$r(eff)_{B-site} = (0.5 - x)\left[r_{Fe^{3+}}\right] + x\left[r_{Sc^{3+}}\right] + 0.5\left[r_{Nb^{5+}}\right] \quad (1)$$

The Shannon ionic radii of Fe^{3+} (low spin), Sc^{3+} and Nb^{5+} are 55 pm, 74.5 pm and 64 pm respectively.[24] Figure 1(b) shows variation of tolerance factor with increasing Sc content. Tolerance factor varies between $1.024 \le t \le 0.976$. However, in literature the crystal systems that possess tolerance factor ($t \ge 0.985$) exhibits a ferroelectric to paraelectric transformation associated with cation displacements.[21,25] In the present study we have observed a clear dependence of structural stabilization with respect to the tolerance factor values as seen in Figure 1(b). In spite of the macroscopic powder diffraction pattern studies the PFSN like compounds are known to exhibit local structural inhomogeneity and hence the electron microscopy study was performed.

TEM bright field image (Fig 2(a)) of $Pb(Sc_{0.5}Nb_{0.5})O_3$ shows the microstructure consisting of submicron sized grains. Interestingly the contrast seen within the single grain is not uniform and indicates presence of domain like microstructure reported for cation ordering in (1-x)$Pb(Mg_{1/3}Nb_{2/3})O_3$–$xPb(Sc_{1/2}Nb_{1/2})O_3$ (PMN–PSN) solid solution system.[26] Note that the dark field imaging using superlattice reflection would be particularly useful to provide direct evidence for the cation ordering induced domain structure formation. The observed faint super lattice reflection hampered such dark field imaging with strong contrast. Nevertheless, the presence of bright and dark regions, appearing within the grain can be attributed to the local compositional heterogeneity

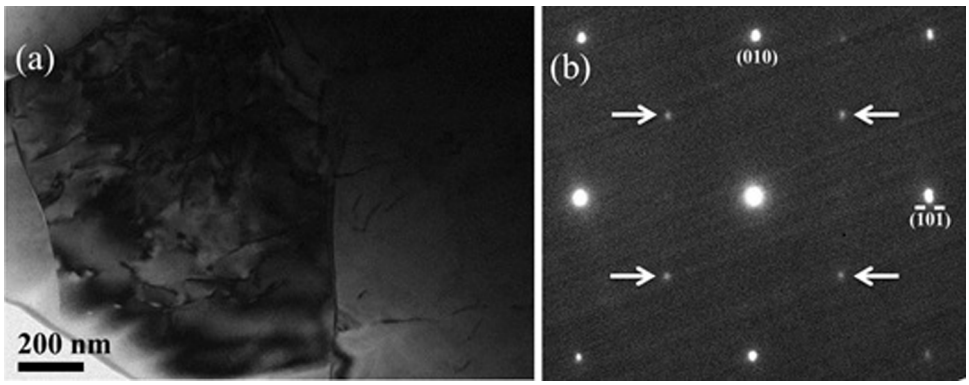

FIG. 2. (a) TEM Bright field image of $Pb(Sc_{0.5}Nb_{0.5})O_3$. The corresponding selected area diffraction pattern recorded along [10$\bar{1}$] zone axis are shown in (b). The additional spots indicated by arrows are superlattice reflection arising from cation ordering.

and cation ordering. Superlattice reflections arising from the ordered regions are evident in the selected area electron diffraction pattern recorded along [10$\bar{1}$] zone axis of cubic perovskite. The observed extra spots correspond to allowed superlattice reflection {h + 1/2, k + 1/2, l + 1/2} for B-site cation ordering and are in agreement with the reported superlattice reflection in $Pb(Sc_{0.5}Ta_{0.5})O_3$.[27] It is interesting to note that the cation ordering evidenced from the superlattice reflection is typically observed for larger content of Sc as confirmed by Raman spectroscopy results and are discussed below with systematic variation in Sc content.

The Raman spectra of all the compounds have been recorded from 300 K – 723 K at different intervals. Phonon modes of Pb based relaxor systems commonly assigned using $Fm\bar{3}m$ space group symmetry in both ferroelectric and paraelectric regime.[19,28–30] In accordance with group theory analysis, the allowed optical phonon modes for this symmetry at the Brillouin zone center includes: $A_{1g} + E_g + 2F_{2g} + 4F_{1u} + F_{2u}$.[19] Among these $A_{1g} + E_g + 2F_{2g}$ are the Raman active modes and the appearance of remaining modes are due to local structural distortions (due to PNRs).[19] Phonon modes in the range of 180-320 cm^{-1} correspond to cation off-center displacements in the PNRs.[28] The prominent phonon modes such as A_{1g} (~800 cm^{-1}), F_{2g} (~550 cm^{-1}), F_{2u} (~350 cm^{-1}), F_{1u} (~260 cm^{-1}) and F_{1g} (~200 cm^{-1}) were assigned with $Fm\bar{3}m$ symmetry, which is conventionally done in PFN and similar structured relaxors.[19,28] Where, A_{1g} mode around 800 cm^{-1} is attributed to the movement of oxygen anions along B′ - O - B″ linkages while remaining cations are at rest.[31] F_{2g} mode around 550 cm^{-1} arises from the symmetric bending of BO_6 octahedra. Modes around 202 cm^{-1}(F_{1g}), 250 cm^{-1} (F_{1u}) corresponds rotation of BO_6 octahedra and B cation ($Fe^{3+}/Nb^{5+}/Sc^{3+}$) localized vibrational modes respectively.[11,12] The mode around 350 cm^{-1} (F_{2u}) is mainly attributed to Pb-O bond stretching due to the electron- phonon coupling of Pb^{2+} lone pair electrons.[11,12] Such mode is known to arise in relaxors that possess cation ordering which leads to strong interaction between the Pb cation and the ferroelectrically active B′, B″ cations. Local cation ordering induced phonon mode such as F_{2u} around 350 cm^{-1} could be seen only in compositions for which $x \geq 0.3$. It is worth remembering that the crystal symmetry of all these compounds ($x \geq 0.3$) is rhombohedral and in addition a B′- B″ cation ordering exists for those compositions that stabilize under rhombohedral symmetry. Such cation ordering was also confirmed from TEM studies shown in figure 2(b). Whereas, due to the absence of B′- B″ cation ordering Pb-O phonon mode expected around 350 cm^{-1} could not seen in compositions with monoclinic symmetry [$0 \leq x \leq 0.25$]. The details of such structurally assisted B′- B″ cation ordering in such compounds has been reported earlier.

De-convolution of all the spectrum has been carried out using *fityk* software[32] with help of voigt profile fitting function. Figure 3(a) – 3(h) shows the de-convoluted spectra of all compounds at three different temperatures (300 K, 523 K and 723 K). Intensity of the all the phonon modes decreases with increasing temperatures as commonly observed in the Raman spectrum of various samples. However, the B-localized (F_{1u}, ~250 cm^{-1}), BO_6 rotational (F_{1g}, ~200 cm^{-1}) phonon modes behave differently with temperature and with composition.

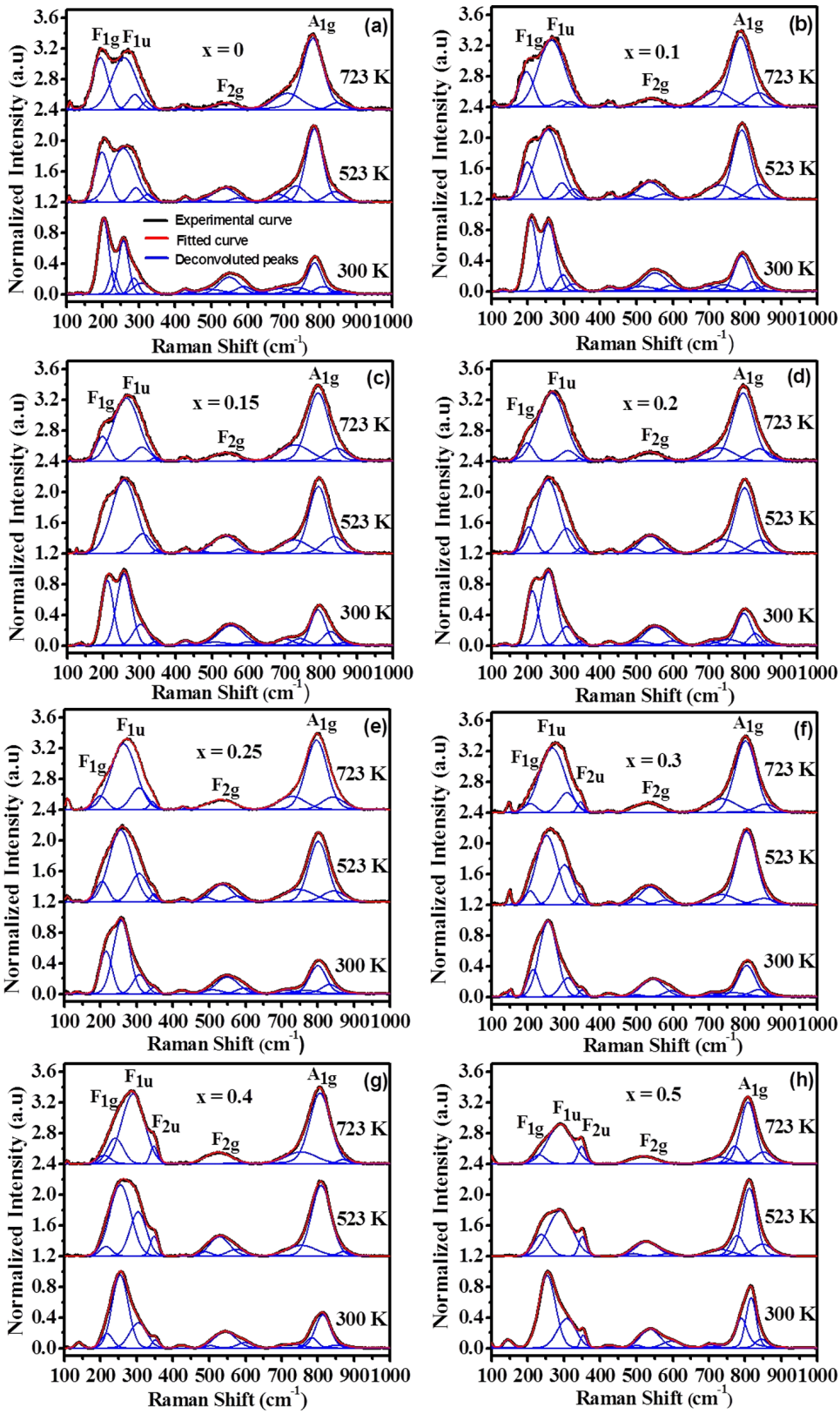

FIG. 3. De-convoluted Raman pectra of $Pb(Fe_{0.5-x}Sc_x)Nb_{0.5}O_3$ compositions with varying x = 0 - 0.5 mol% of Sc recorded at three different temperatures 300 K, 523 K and 723 K [Note: The labeling mentioned in figure 3(a) for different colors is applicable to all the compositions of this figure 3].

In PFSN like relaxors, the ferroelectrically active B″ cation and the respective BO_6 octahedral modes play a crucial role in ferroelectric nature of the system. Figure 4 shows the temperature variation of B-localized (F_{1u}, ~250 cm^{-1}), and BO_6 rotational modes (F_{1g}, ~200 cm^{-1}) which originates due to structural distortions associated with polar nano regions.[2,3,28] B-localized mode (F_{1u}) softens with increasing temperature until T_m (temperature corresponding to dielectric maxima), beyond which it hardens in all the compositions of PFSN (see Fig 4(a) – 4(h). Hence, it is evident that the B-localized phonon mode does get affected across the ferroelectric phase transition. It is also known that for perovskite systems that possess tolerance factor ≤ 0.98 involves octahedral tilt

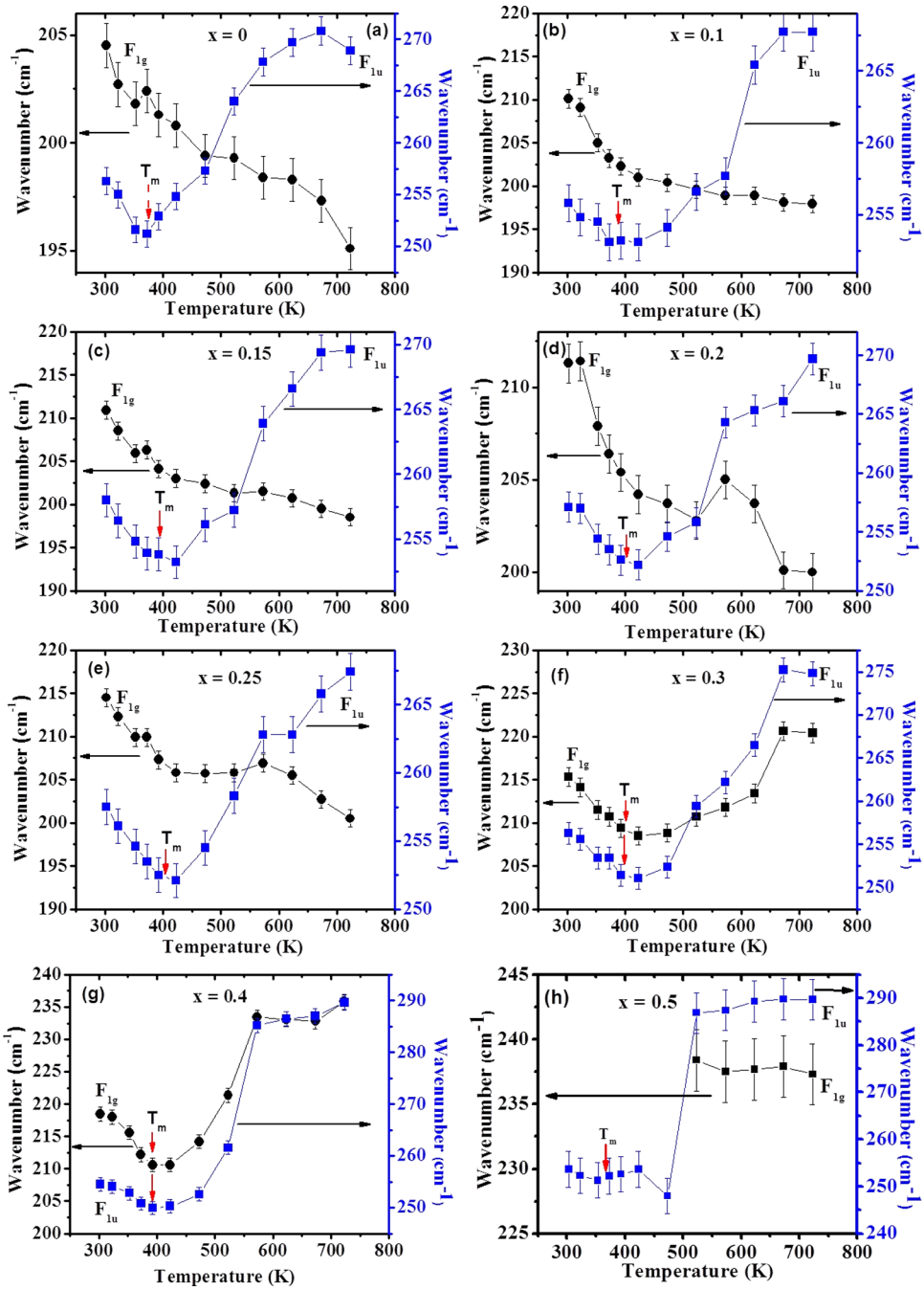

FIG. 4. Temperature dependence of BO_6 rotational mode (F_{1g}) and B-localized (F_{1u}) in $Pb(Fe_{0.5-x}Sc_x)Nb_{0.5}O_3$ compounds with x varying from 0.0 to 0.5.

movements across the structural transformation.[21] Whereas, in systems with tolerance factor value ≥ 0.98 cation off center displacements play crucial role across the structural transformation.[21] The observed behavior of B-localized mode in all the compositions studied (value of tolerance factor lies in between 0.97-1.024) corroborates well with the B-cation off center displacements involved across the structural transformation.

Interestingly, BO_6 rotational mode (F_{1g}, ~200 cm^{-1}) softens with increasing temperature and follows the similar trend across and beyond T_m in all the compositions with monoclinic (Cm) symmetry ($0 \le x \le 0.25$). But in the case of PFSN with composition value of ($0.3 \le x \le 0.5$) possessing Rhombohedral (R3m) symmetry both the B localized mode and the BO_6 rotational mode has a similar behavior both below and above T_m [figure 4(f)-4(h)]. In pure PSN (x = 0.5) compound (Figure 4(h)) those modes could be distinctly identified only well above the T_m. Such correlated behavior between B-localized and BO_6 rotational mode could arise due to the crystal structure assisted B′-B″ cation ordering. It is worth remembering that there is a 34-36% increment in the unit cell volume and a reduction in $B'/B'' - O - B'/B''$ bond angle, which might also assist such correlation between B-localized and BO_6 rotational modes. The presence of such structure and cationic order assisted phonon correlation should eventually increase the interaction among the PNRs. Under such conditions, correlation between the lattice modes might reflect on the macroscopic dielectric phase transition behavior. In order to study the influence of these correlated phonon modes on the macroscopic phenomenological behavior the temperature dependent dielectric studies of PFSN ceramics at different probe frequency were carried out.

Figure 5(a) – 5(c) shows the variation of relative permittivity with temperature for selected compositions; x = 0, x = 0.25, x = 0.5. The phase transition behavior is diffused, which is a common feature of these complex oxides. The order of diffusivity could be estimated through the modified Curie Weiss Law given in equation (2).[33,34]

$$\frac{1}{\varepsilon'} - \frac{1}{\varepsilon'_{max}} = \frac{(T - T_m)^{\gamma}}{C'} \tag{2}$$

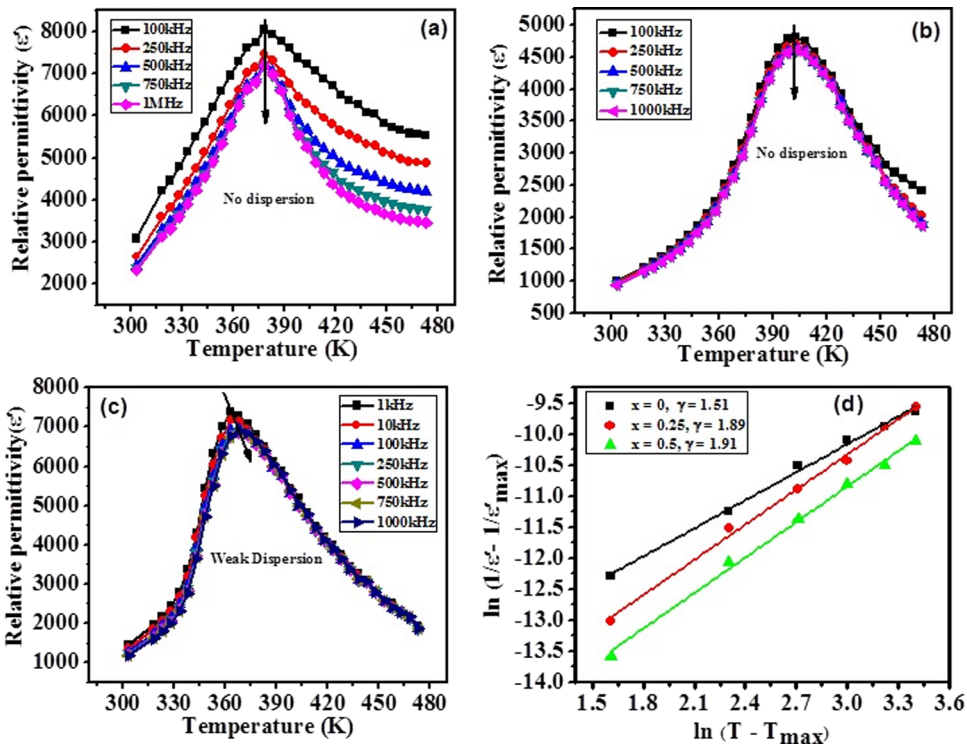

FIG. 5. Variation of dielectric permittivity with temperature for three selected compositions: (a) $Pb(Fe_{0.5}Nb_{0.5})O_3$ (b) $Pb(Fe_{0.25}Sc_{0.25}Nb_{0.5})O_3$ (c) $Pb(Sc_{0.5}Nb_{0.5})O_3$ (d) Modified Curie Weiss plot of three selected compositions.

Here, ε' real part of dielectric permittivity, ε'_{max} maximum value of real part of dielectric permittivity, T_m is the temperature at which maximum ε', γ is the diffusivity parameter and C′ is modified curie constant. The diffusivity parameter $\gamma = 1$ for normal ferroelectrics, $\gamma = 2$ for relaxor ferroelectrics. Figure 5(d) shows variation of $\ln(1/\varepsilon' - 1/\varepsilon'_{max})$ as a function of $\ln(T - T_m)$ estimated at 1MHz for three selective compositions (x = 0, 0.25, 0.5). The slope of linear fit of plot (figure 5(d)) gives the diffusivity parameter of the respective compound. The diffusivity of $Pb(Fe_{0.5}Nb_{0.5})O_3$ ($\gamma = 1.51$) might be because of compositional fluctuations and it does not exhibit any relaxor features. Whereas, the high diffusivity values of $Pb(Fe_{0.25}Sc_{0.25}Nb_{0.5})O_3$ ($\gamma = 1.88$) and $Pb(Sc_{0.5}Nb_{0.5})O_3$ ($\gamma = 1.91$) attributed to relaxor feature. Most importantly, a weak frequency dispersion in the T_m is observed in $Pb(Sc_{0.5}Nb_{0.5})O_3$ (x = 0.5) exhibiting rhombohedral symmetry is attributed to structurally driven B′-B″ cation ordering. As discussed earlier, this composition also exhibits a correlation between B-localized and BO_6 rotational phonon modes across the ferroelectric phase transformation. Thus, the structure and cation order assisted strong correlation between B-localized and BO_6 rotational phonon modes increases interaction between PNRs, which results in diffusive and dispersive ferroelectric phase transformation.

IV. CONCLUSION

In conclusion, $Pb(Fe_{0.5-x}Sc_xNb_{0.5})O_3$ ($0 \le x \le 0.5$) ceramics with increasing Sc content undergoes a structural transformation from monoclinic (Cm) to rhombohedral (R3m) at x = 0.3. The transformation is also associated with 34-36% of increment in the unitcell volume and reduction in $B'/B'' - O - B'/B''$ bond angle from $\approx 175°$ to 153°. The TEM studies confirm the existence of B′ and B″ cation ordering in PSN with rhombohedral symmetry. From the investigation of high temperature Raman spectra B-localized (250 cm^{-1}) and BO_6 rotational (200 cm^{-1}) modes exhibit clear distinction between the monoclinic and rhombohedral symmetry. In the case of rhombohedral symmetry a correlated behavior both below and above T_m was observed. The effect of such phonon correlation is evidently seen in the macroscopic dielectric phase transition behavior of PSN. However, all the compositions exhibited a broad diffusive transformation and the diffusivity values obtained from modified Curie-Weiss plot reveal those compositions with the correlated phonon behavior exhibits relatively larger diffusive nature and a weak dispersion in T_m in the phase transformation.

ACKNOWLEDGEMENT

One of the authors R Ranjith would like to acknowledge DST-India Fast Track scheme (Project No: SR/FTP/PS-170/2012) for the funding of the project. Another author B Mallesham would like to thank Ministry of Human Resource Development (MHRD), Government of India for providing fellowship.

[1] A. M. Welsch, B. Mihailova, M. Gospodinov, R. Stosch, B. Guttler, and U. Bismayer, J. Phys: Condens. Matter **21**, 235901 (2009).
[2] B. Maier, B. Mihailova, C. Paulmann, J. Ihringer, M. Gospodinov, R. Stosch, B. Guttler, and U. Bismayer, Phys. Rev. B **79**, 224108 (2009).
[3] B. J. Maier, A. M. Welsch, B. Mihailova, R. J. Angel, J. Zhao, C. Paulmann, J. M. Engel, W. G. Marshall, M. Gospodinov, D. Petrova, and U. Bismayer, Phys. Rev. B **83**, 134106 (2011).
[4] O. Svitelskiy, J. Toulouse, G. Yong, and Z. G. Ye, Phys. Rev. B **68**, 104107 (2003).
[5] B. Mallesham, R. Ranjith, and M. Manivelraja, J. Appl. Phys. **116**, 034104 (2014).
[6] I. W. Chen, P. Li, and Y. Wang, J. Phys. Chem. Solids. **57**, 1525 (1996).
[7] C. A. Randall, A. S. Bhalla, T. R. Shrout, and L.E. Cross, J. Mater. Res. **5**, 829 (1990).
[8] G. Burns and F. H. Dacol, Ferroelectrics **104**, 25 (1990).
[9] B. P. Burton, E. Cockayne, and U. V. Waghmare, Phys. Rev. B **72**, 064113 (2005).
[10] M. Pasciak, T. R. Welberry, J. Kulda, M. Kempa, and J. Hlinka, Phys. Rev. B **85**, 224109 (2012).
[11] B. Mihailova, U. Bismayer, B. Guttler, M. Gospodinov, A. Boris, C. Berndhard, and M. Aroyo, Z. Kristallogr. **220**, 740 (2005).
[12] B. Guttler, B. Mihailova, R. Stosch, U. Bismayer, and M. Gospodinov, J. Mol. Struct. **661**, 469 (2003).
[13] D. I. Khomskii, J. Magn. Magn. Mater. **306**, 1 (2006).
[14] G. A. Smolenskii, A. Agranovskaya, S. N. Popov, and V. A. Isupov, Sov. Phys. Tech. Phys. **28**, 2152 (1958).

[15] A. Kumar, R. S. Katiyar, C. Rinaldi, S. G. Lushnikov, and T. A. Shaplygina, Appl. Phys. Lett. **93**, 232902 (2008).
[16] O. Raymond, R. Font, N. Suarez-Almodovar, J. Portelles, and J. M. Siqueiros, J. Appl. Phys. **97**, 084107 (2005).
[17] R. Blinc, P. Cevc, A. Zorko, J. Holc, M. Kosec, Z. Trontelj, J. Pirnat, N. Dalal, V. Ramachandran, and J. Krzystek, J. Appl. Phys. **101**, 033901 (2007).
[18] Y. Yang, J. M. Liu, H. B. Huang, W. Q. Zou, P. Bao, and Z. B. Liu, Phys. Rev. B. **70**, 132101 (2004).
[19] D. P. Kozlenko, S. E. Kichanov, E. V. Lukin, N. T. Dang, L. S. Dubrovinsky, H. P. Liermann, W. Morgenroth, A. A. Kamynin, S. A. Gridnev, and B. N. Savenko, Phys. Rev. B **89**, 174107 (2014).
[20] W. C. Lee, C. Y. Huang, L. K Tsao, and Y. C. Wu, J. Eur. Ceram. Soc. **29**, 1443 (2009).
[21] I. M. Reaney, E. L. Colla, and N. Setter, Jpn. J. Appl. Phys. **33**, 3984 (1994).
[22] M. R. Suchomel and P. K Davies, J. Appl. Phys. **96**, 4405 (2004).
[23] N. Vittayakorn, G. Rujijanagul, T. Tunkasiri, X. Tan, and D. P. Cann, J. Mater. Res **18**, 2282 (2003).
[24] R. D. Shannon, Acta Cryst.A. **32**, 751 (1976).
[25] P. G. Fernandez, J. A. Aramburu, M. T. Barriuso, and M. Moreno, J. Phy. Chem. Lett. **1**, 647 (2010).
[26] L. Farber, M. Valant, M. A. Akbas, and P. K. Davies, J. Am. Ceram. Soc. **85**, 2319 (2002).
[27] D. Liu and D. A. Payne, J. Appl. Phys. **77**, 3361 (1995).
[28] M. Correa, A. Kumar, S. Priya, R. S. Katiyar, and J. F Scott, Phys. Rev. B **83**, 014302 (2011).
[29] N. Waeselmann, B. Mihailova, B. J. Maier, C. Paulmann, G. Gospodinov, V. Marinova, and U. Bismayer, Phys. Rev. B **83**, 214104 (2011).
[30] D.K. Pradhan, S. Sahoo, S. K. Barik, V. S. Puli, P. Misra, and R. S. Katiyar, J. Appl. Phys. **115**, 194105 (2014).
[31] D. Rout, V. Subramanian, K. Hariharan, and V. Sivasubramanian, Solid State Commun. **141**, 192 (2007).
[32] M. Wojdyr, J. Appl. Cryst. **43**, 1126 (2010).
[33] Z. Y. Cheng, R. S. Katiyar, X. Yao, and A. Guo, Phys. Rev. B **55**, 8165 (1997).
[34] Z. Yu, C. Ang, R. Guo, and A. S. Bhalla, J. Appl. Phys. **92**, 2655 (2002).